



Which modality is better to diagnose high-grade transformation in retroperitoneal liposarcoma? Comparison of computed tomography, positron emission tomography, and magnetic resonance imaging

Yu Nakashima¹ · Yukihiro Yokoyama¹ · Hiroshi Ogawa² · Ayako Sakakibara³ · Masaki Sunagawa¹ · Yoshihiro Nishida⁴ · Takashi Mizuno¹ · Junpei Yamaguchi¹ · Shunsuke Onoe¹ · Nobuyuki Watanabe¹ · Shoji Kawakatsu¹ · Tsuyoshi Igami¹ · Tomoki Ebata¹

Received: 5 September 2022 / Accepted: 20 December 2022 / Published online: 30 December 2022
© The Author(s) under exclusive licence to Japan Society of Clinical Oncology 2022

Abstract

Background Survival in patients with retroperitoneal liposarcoma (RPLS) depends on the surgical management of the dedifferentiated foci. The present study investigated the diagnostic yield of contrast-enhanced CT, ¹⁸F-fluorodeoxyglucose positron emission tomography (PET), and diffusion-weighted MRI in terms of dedifferentiated foci within the RPLS.

Methods Patients treated with primary or recurrent RPLS who underwent the above imaging between January 2010 and December 2021 were retrospectively reviewed. The diagnostic accuracy of the three modalities for histologic subtype of dedifferentiated liposarcoma (DDLs) and French Federation of Cancer Center (FNCLCC) grade 2/3 were compared using receiver operating characteristic curves and areas under the curves (AUCs).

Results The cohort involved 32 patients with 53 tumors; 30 of which exhibited DDLs and 31 of which did FNCLCC grades 2/3. The optimal thresholds for predicting DDLs were mean CT value of 31 Hounsfield Unit (HU) (AUC=0.880, 95% CI 0.775–0.984; $p < 0.001$), maximum standardized uptake value (SUVmax) of 2.9 (AUC = 0.865 95% CI 0.792–0.980; $p < 0.001$), while MRI failed to differentiate DDLs. The cutoff values for distinguishing FNCLCC grades 1 and 2/3 were a mean CT value of 24 HU (AUC = 0.858, 95% CI 0.731–0.985; $p < 0.001$) and SUVmax of 2.9 (AUC = 0.885, 95% CI 0.792–0.978; $p < 0.001$). MRI had no sufficient power to separate these grades.

Conclusions Contrast-enhanced CT and PET were useful for predicting DDLs and FNCLCC grade 2/3, while MRI was inferior to these two modalities.

Keywords Retroperitoneal liposarcoma · Differentiation · Imaging analysis · ¹⁸F-fluorodeoxyglucose positron emission tomography · Diffusion-weighted MRI

Introduction

Retroperitoneal liposarcoma (RPLS) is the most common malignant tumor occurring in the retroperitoneal space, accounting for approximately 15% of all soft-tissue sarcomas in adults [1, 2]. Complete surgical resection is a mainstay in the treatment of RPLS because chemotherapy or radiotherapy is generally ineffective for this disease [1]. In particular, resection of the dedifferentiated component of RPLS with a negative surgical margin is essential to achieve better local recurrence-free survival after surgery [3]. RPLS is frequently found as an extra-large tumor that occupies the entire retroperitoneal space, and it commonly exhibit a

✉ Yukihiro Yokoyama
yyoko@med.nagoya-u.ac.jp

¹ Division of Surgical Oncology, Department of Surgery, Nagoya University Graduate School of Medicine, 65 Tsurumai-cho, Showa-ku, Nagoya, Aichi 466-8550, Japan

² Department of Radiology, Nagoya University Graduate School of Medicine, Nagoya, Japan

³ Department of Pathology and Laboratory Medicine, Nagoya University Hospital, Nagoya, Japan

⁴ Department of Orthopedics, Nagoya University Graduate School of Medicine, Nagoya, Japan

heterogeneous tumor appearance including well-differentiated and dedifferentiated histology. Unclear gross tumor border of the dedifferentiated part often end in positive margin, which substantially worsens survival as well as local control after surgery [3]. In this regard, pinpointing the dedifferentiated foci is a key element toward successful resection.

Computed tomography (CT), ^{18}F -fluorodeoxyglucose positron emission tomography (PET), and magnetic resonance imaging (MRI) are three major imaging modalities that are used in the diagnosis of RPLS. In general, CT determines the precise anatomic location, vascularity (when contrast medium is used), size, and invasion. In contrast, PET inspects the functional capacity of glucose metabolism of the tumor. MRI delineates the histologic cellularity of the tumor and its association with surrounding tissue.

Several studies have reported the usefulness of CT for identifying dedifferentiated components [4, 5], while, other studies showed the utility of PET imaging using a specific cutoff value of the SUVmax [6–8]. Studies investigating the detectability of MRI for dedifferentiated components are sparse, whereas many studies addressed that ADCmap obtained from diffusion-weighted MRI is correlated with neoplastic lesion aggressiveness [9–11]. As discussed so far, the authors hypothesized that ADCmap may be useful in identifying dedifferentiated components of RPLS. However, the diagnostic accuracy of these three modalities against the dedifferentiated component has not been compared previously. The aim of the present study was to determine the most optimal imaging modality to specify the dedifferentiation nature in the complex morphology of RPLS.

Patients and methods

Patients

All patients who underwent CT, PET, and MRI for the diagnosis of primary or recurrent RPLS between January 2010 and December 2021 in Nagoya University Hospital were included in the study. The presence of RPLS was histologically confirmed by the examination of specimens obtained through surgical resection. In the present study, some patients had multiple tumors. If multiple tumors were isolated radiologically and macroscopically with definite histologic diagnosis for each, the tumors were treated as independent tumor in this study. In addition, dedifferentiated tumors that had an encapsulating boundary to well-differentiated component were counted as discrete tumor. Patients with the following conditions were excluded: MRI scan in an inappropriate range, unknown histologic diagnosis because of high heterogeneity, chemotherapy treatment before surgery or biopsy, and small tumors that were not identifiable on the ADC map.

Patient demographic characteristics, pathologic features, and radiological findings were collected from the institutional clinical database. This study was approved by the Human Research Review Committee of Nagoya University Hospital (Approval Number: 2019–0236).

Histologic diagnosis

According to the WHO classification of soft tissue tumors [12], histologic types of liposarcoma were classified as follows: well-differentiated liposarcoma (WDLS), dedifferentiated liposarcoma (DDLs), myxoid liposarcoma (MLS), pleomorphic liposarcoma (PLS), and myxoid pleomorphic liposarcoma (MPLS). In the present study, there were no patients with the latter three histologies. Pathological diagnosis was made by two or more pathologists in all cases.

The French Federation of Cancer Center (FNCLCC) grading system [13] was also used for evaluating histologic malignant potential. The FNCLCC grading system is rated with the total of the scores for three parameters: tumor differentiation, degree of necrosis, and mitotic count. The grading in the present study was performed by one pathologist. The cohort in the present study was separated into two groups depending on the histologic malignancy: FNCLCC system grade 1 and grade 2/3.

Enhanced CT scan protocol

Contrast-enhanced CT was performed using one of the following 3 systems: a 64-detector-row CT system (Aquilion [Canon Medical Systems]), 320-detector-row CT system (Aquilion ONE [Canon Medical Systems]), 160-detector-row CT system (Aquilion Precision [Canon Medical Systems]), or 64-detector-row Dual Source CT system (SOMATOM Definition Flash [Siemens Medical Systems]). The contrast medium used was composed of the following: 100 mL of Omnipaque 300 (GE healthcare Japan) at an infusion rate of 3.3 mL/s for patients weighing less than 45 kg, 120 mL at 4 mL/s for those weighing 45 to 55 kg, and 150 mL at 5 mL/s for those weighing 55 kg or more. After the intravenous injection of contrast medium, 25 mL of saline was injected in 5 s. Images were acquired immediately before contrast medium administration (simple phase) and 25, 45, 70, and 150 s after administration (early arterial, late arterial, portal-venous, and delayed phases, respectively).

FDG-PET protocol

A whole-body PET scanner (Siemens Biograph 16) was used for the PET studies performed in our institution. Patients were imaged after fasting for a minimum of 6 h except for water and medications, providing serum glucose levels were less than 200 mg/dL. ^{18}F -Fluorodeoxyglucose

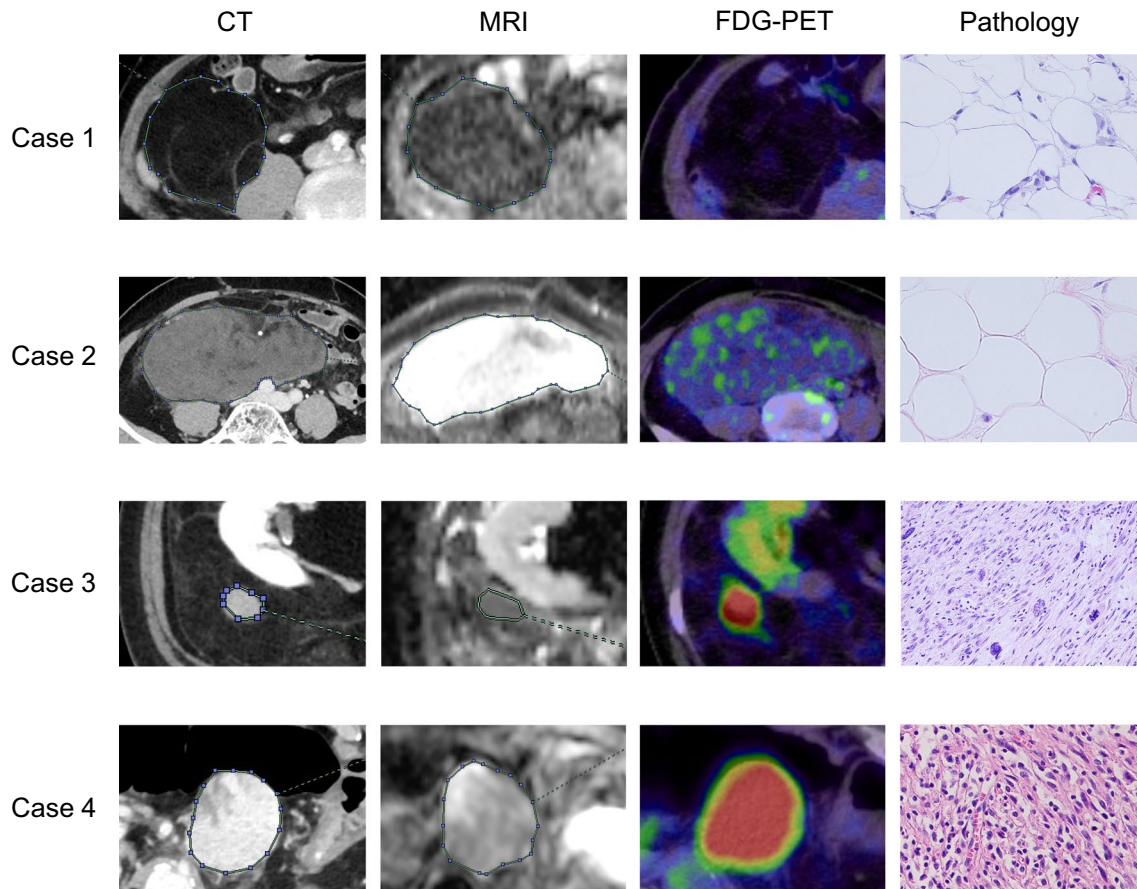


Fig. 1 Examples of how the ROIs were drawn in CT, PET-CT, MRI, and pathological specimens: hematoxylin–eosin 100× magnification. Case 1: A 73-year-old man with WDLs. On CT, the tumor has a very low density, similar to that of normal fat tissue. The ADC map showed an uneven tumor with very low signal intensity and a slightly hazy border. Case 2: A 70-year-old man with WDLs. This large tumor was uneven and showed slightly high density on CT. The ADC map showed a very high signal intensity. The tumor was well circumscribed. Case 3: A 40-year-old woman with DDLS. Most of

the tumors consisted of WDLs. A small area with very high density was found in a large well-differentiated tumor on CT. In this area, the ADC value was low on the ADC map, and the SUVmax was very high on PET-CT. The boundary was unclear on ADCmap, and the ROI on ADC map was drawn with reference to the area of SUVmax. Case 4: A 77-year-old man with DDLS. A well-circumscribed and uneven tumor was imaged and showed high density on CT and low signal intensity on ADC map. PET-CT showed a very high SUVmax

(^{18}F -FDG) was injected intravenously in doses of 3.7 MBq/kg for patients weighing less than 60 kg and 4.07 MBq/kg for those weighing 60 kg or more. Whole-body imaging commenced 60 min after the injection of ^{18}F -FDG. Imaging was performed at each level from the head to the upper thigh. Some studies were performed at an institution where the images were imported and reviewed.

MRI protocol

MRI was performed using one of the following 6 systems: a 1.5-T scanner (Magnetom Aera, Magnetom Avanto-SQ [Siemens Medical Systems]), 3.0-T scanner (Magnetom Skyra, Magnetom Verio, Magnetom Prisma [Siemens Medical Systems]), or Vantage Centurian [Canon Medical Systems]). A routine MRI protocol was applied to all patients, including

axial and coronal T2-weighted imaging, axial T1-weighted imaging, and axial DWI with no contrast-enhanced imaging. ADC maps were generated using DWIs with b values of 0 and 1000 s/mm^2 .

Image analysis

First, SUVmax of each tumor was calculated automatically using volume of interest segmentation of the lesion on PET imaging. Mean CT values were manually obtained from regions of interests (ROIs) that were placed at the same level and in the same position as the area of SUVmax at axial PET. This process was performed on the portal-venous phases in all patients. In the case of tumors that have uneven components, ROIs were set with reference to the point of SUVmax in the tumor. In MRI image analysis, the

Table 1 Characteristics of patients and tumors in this study

Number of tumors	53
Number of patients	32
Age [years], median (IQR)	56 (54–71)
Sex, male, <i>n</i> (%)	16 (50.0)
Body mass index [kg/m ²], median (IQR)	22.9 (19.0–25.1)
Maximum diameter of tumor [mm], median (IQR)	50 (25–105)
Tumor status, <i>n</i> (%)	
Primary	26 (49.1)
Recurrence	27 (50.9)
Histological subtype, <i>n</i> (%)	
Well differentiated	23 (43.4)
Dedifferentiated	30 (56.6)
FNCLCC grade, <i>n</i> (%)	
Grade 1	22 (41.5)
Grade 2	28 (52.8)
Grade 3	3 (5.7)
Mean CT value [HU], median (IQR)	48 (– 8–78)
SUV max, median (IQR)	3.75 (2.50–6.49)
Mean ADC value [$\times 10^{-3}$ mm ² /s], median (IQR)	1.28 (0.99–1.69)

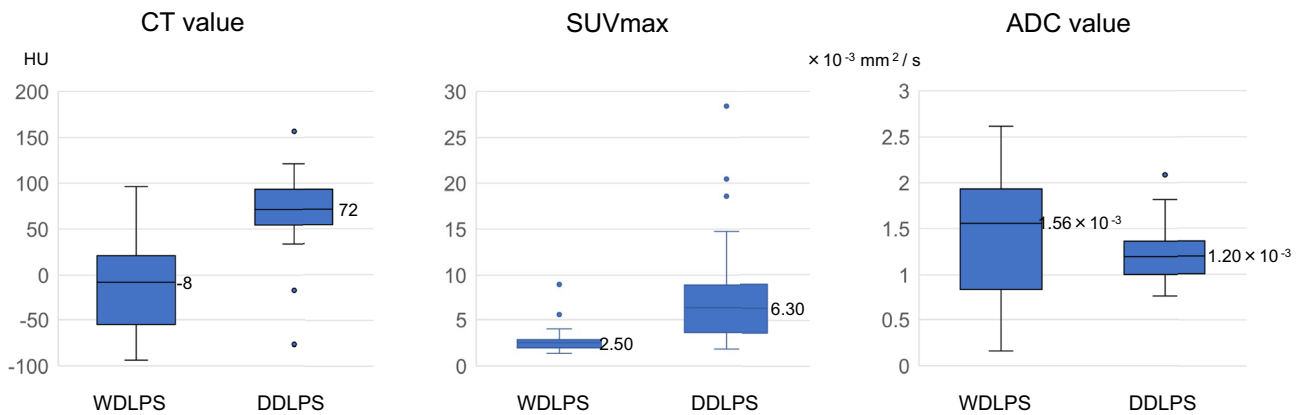
mean ADC value was calculated on the same ROIs in CT image analysis. All ROI assignments were performed with

a consensus decision by two observers (Y.N and Y.Y). All image analysis mentioned above were conducted using an image analysis software Synapse Vincent 3D Image Analysis System (Fujifilm Corporation, Tokyo, Japan).

Examples of how ROIs were drawn in CT, PET-CT, and MRI are described in Fig. 1. In case 1, the median value of the mean CT value, SUVmax, and mean ADC value were -94 HU, 1.97, and 0.55×10^{-3} mm²/s, respectively.

Statistical analysis

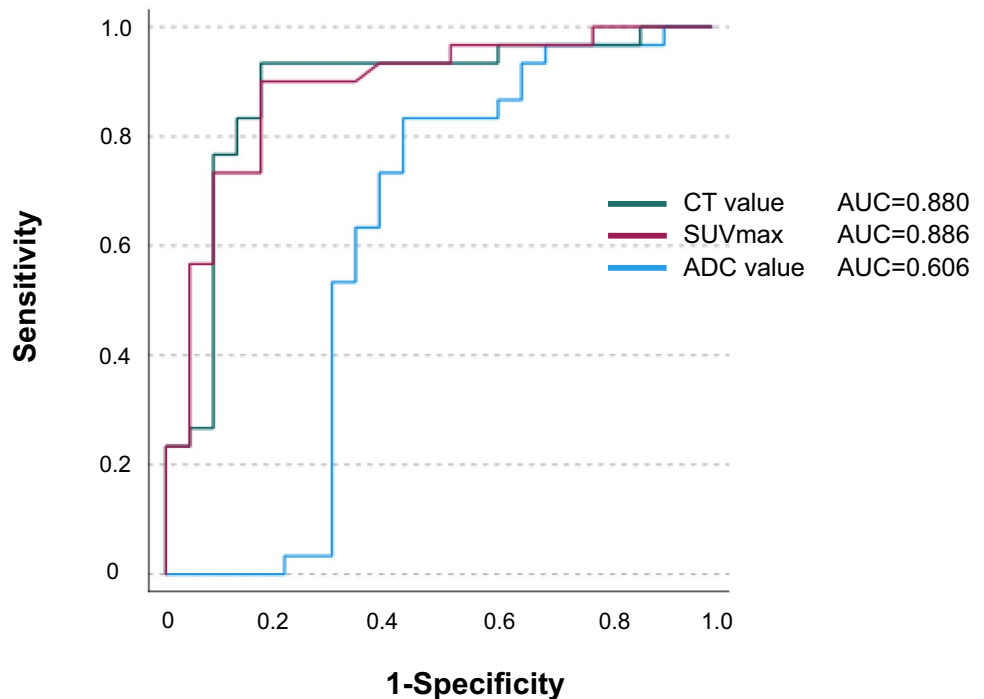
Continuous data are expressed as medians with interquartile ranges. Statistical analyses were performed using a Mann–Whitney U test for the difference between two continuous variables. Using the data of the mean CT value, SUVmax, and mean ADC value collected and measured by the method described above, receiver-operating characteristic (ROC) curves were generated, and areas under the curves (AUCs) were calculated for the prediction of the dedifferentiated component and FNCLCC grade 2/3. The optimal threshold cutoff values of the mean CT value, SUVmax, and mean ADC to distinguish whether the lesion of the tumor was WDLs or DDLs/FNCLCC grade 1 or 2/3 were determined along with sensitivity and specificity. The predictive accuracies of the mean CT value, SUVmax, and mean ADC



		WDLPS	DDLPS	p value
CT value (HU)	median (IQR)	-8 (-46 - 18)	72 (58- 90)	<0.001*
SUVmax	median (IQR)	2.50 (2.04 - 2.81)	6.30 (3.86 - 8.78)	<0.001*
ADC value ($\times 10^{-3}$mm²/s)	median (IQR)	1.56 (0.89 - 1.89)	1.20 (1.02 - 1.36)	0.190

Fig. 2 Distribution of the CT value, SUVmax and ADC value by pathological diagnosis

Fig. 3 ROC curve for CT value, SUVmax and ADC value in discriminating between DDLS and WDLS. CT and PET had enough power to distinguish between DDLS and WDLS, while MRI did not.



AUC difference

CT vs PET-CT	0.006	$p = 0.865$
CT vs MRI	0.274	$p = 0.003$
PET-CT vs MRI	0.270	$p = 0.002$

Cut-off point

CT value	30.76 HU
SUVmax	2.895
ADC value	$1.44 \times 10^{-3} \text{ mm}^2/\text{s}$

value were compared using the χ^2 test for differences in the AUCs. All tests of significance used a two-sided p value less than 0.05. Statistical calculations were performed using IBM SPSS Statistics® version 28 (IBM Japan Inc., Tokyo, Japan).

Results

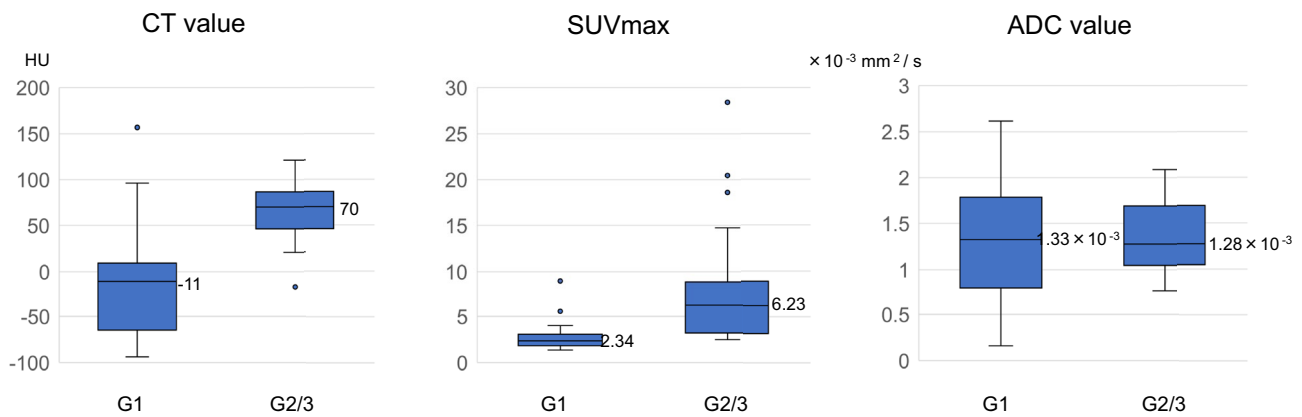
Baseline characteristics of patients and tumors

The study cohort consisted of 32 patients and 53 tumors (Table 1). Of the 53 tumors, 23 (43%) were WDLS, and 30 (57%) were DDLS. The FNCLCC score was grade 1 in 22 tumors (42%), grade 2 in 28 tumors (53%), and grade 3 in 3 tumors (5.7%).

Predictive availability of the mean CT value and SUVmax for histologic subtypes and FNCLCC grades

CT and PET showed significant difference between WDLS and DDLS, while MRI did not (Fig. 2). On the ROC curve analysis, a mean CT value of 31 HU provided an optimal threshold to discriminate between the two tumor types (AUC = 0.880, 95% CI 0.775–0.984; $p < 0.001$), yielding 90% sensitivity and 83% specificity for DDLS (Fig. 3). Likewise, an SUVmax of 2.9 (AUC = 0.865 95% CI 0.792–0.980; $p < 0.001$) had 90% sensitivity and 83% specificity.

As for FNCLCC grades, CT and PET had enough discriminatory power between grade 1 and grade 2/3, whereas MRI



		G1	G2/3	p value
CT value (HU)	median (IQR)	-11 (-61 - 8)	70 (47- 84)	<0.001*
SUVmax	median (IQR)	2.34 (1.87 - 2.82)	6.23 (3.22 - 8.67)	<0.001*
ADC value ($\times 10^{-3}\text{mm}^2/\text{s}$)	median (IQR)	1.33 (0.86 - 1.74)	1.28 (1.06 - 1.54)	0.942

Fig. 4 Distribution of CT value, SUVmax and ADC value by FNCLCC grades 1 and 2/3

had no sufficient power to separate these grades (Fig. 4). On the ROC curve analysis, the cutoff value in CT was set at 24 HU (AUC = 0.858, 95% CI 0.731–0.985; $p < 0.001$), yielding 97% sensitivity and 82% specificity. Meanwhile, the cutoff value in SUVmax was 2.9 (AUC = 0.885, 95% CI 0.792–0.978; $p < 0.001$), yielding 84% sensitivity and 77% specificity (Fig. 5).

Discussion

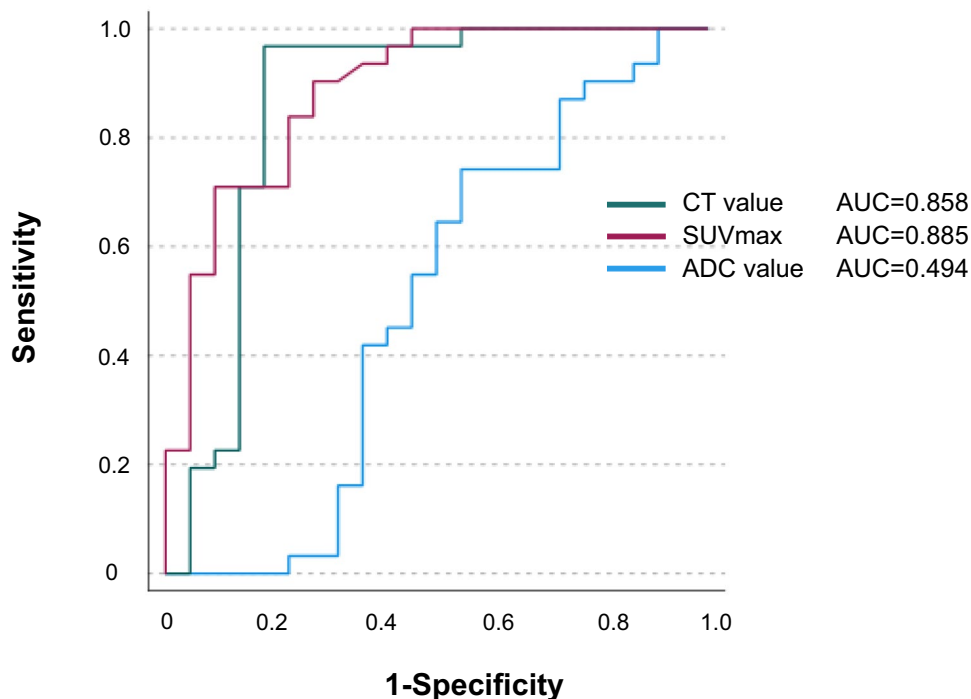
Biologic behavior of RPLS exhibits heterogeneity, depending on tumor histology. Well-differentiated histology shows a less aggressive nature with frequent local relapse and rare distant metastasis after surgery. In contrast, dedifferentiated tumor has a high incidence of local recurrence and distant metastasis [14–21], indicating a clinically aggressive form. Unfortunately, the latter tumor type occurs spontaneously inside the well-differentiated tumor with tumor progression or during therapeutic course, making the tumor morphology complex. Preoperative histologic confirmation may guide surgeons to design an appropriate surgical approach to maximize the chance of curative resection against dedifferentiated tumor transformation. Therefore, we think that the

presurgical radiologic diagnosis for this challenging tumor improves the prognosis of patients with RPLS.

In this study, we evaluated the diagnostic accuracy of MRI (using ADCmap) for the dedifferentiated component of RPLS because MRI has a great advantage over CT or PET: no radiation exposure. However, in contrast to our expectation, the detectability of MRI was inferior to both CT and PET. This may be attributed to the low spatial resolution and intense signal noise of ADCmap. ADCmap is computed from two or more b values. Hence, the presence of misalignment between images at different b values potentially includes imprecision and discrepancy for tumor location. More accurate methods to estimate ADC values have been reported in some studies [22–24], but they are not practical for RPLS due to the necessity of complex imaging technology with advanced radiological knowledge.

Our study revealed that CT and PET had a good discriminatory ability to check dedifferentiated foci, and there was no significant difference in the power between the two modalities. PET is useful for evaluating biological malignant potential in various neoplasms and detecting unexpected distant metastases. Thus, our findings demonstrating an equivalent diagnostic power of PET to CT suggest that PET may not always be mandatory prior to resection for

Fig. 5 ROC curve for CT value, SUVmax and ADC value in discriminating FNCLCC grades 1 and 2/3. CT and PET had enough power to distinguish between FNCLCC grades 1 and 2/3, but MRI was not significantly sufficient.



AUC difference

CT vs PET-CT	0.028	p= 0.601
CT vs MRI	0.364	p< 0.001
PET-CT vs MRI	0.391	p< 0.001

Cut-off point

CT value	24.41 HU
SUVmax	2.895
ADC value	$1.44 \times 10^{-3} \text{ mm}^2/\text{s}$

RPLS. Omitting PET in routine workup of RPLS renders cost-friendly, patient-friendly, and environment-friendly [25]. It should be noted, however, that PET with SUVmax is necessary to estimate the biological effect by radiation or chemotherapy, because downsize of the tumor is exceptionally gained in RPLS.

CT and MRI had high sensitivity and specificity in identifying DDLS with the cutoff values as follows: CT value of 31 HU, SUVmax of 2.9. Several studies have reported that morphologic CT finding including inside calcification, enhancing deposit, hypervascularity, and necrosis might be useful for identifying dedifferentiated components [4, 5]. These findings are often detectable with plain CT, but it is difficult to accurately diagnose dedifferentiated tumors

that do not have nonfatty component and/or calcification by plain CT. Thus, we used contrast-enhanced CT in the present study. However, CT values of tumors calculated from ROIs have not been appraised yet. Therefore, as far as we know, this is the first study to provide a specific cutoff CT value for radiologic surveillance for DDLS. A few studies have recently addressed that PET worked as an effective diagnostic tool for identifying histologic subtypes of RPLS in which cutoff value of SUVmax was set at 3.8 or 4.0 [6, 7]. Nevertheless, these studies did not compare the diagnostic accuracy between PET and CT or MRI. In this regard, this clearly demonstrated the diagnostic accuracy of these three modalities through ROC curve analysis.

Similar to the differentiation of WDLS and DDLS, CT and PET showed a favorable sensitivity and specificity for the differentiation of FNCLCC histologic grade. However, MRI was not useful in differentiating histologic subtype and grade. In general, ADCmap is considered a useful tool in detecting tumor cellularity, which may be related to the aggressiveness and malignant potential in various cancers [26–30]. However, at least in this study, ADCmap was less useful in distinguishing histologic type as well as histologic grade in RPLS. The reason for the inferior histologic diagnostic accuracy of MRI was not clarified in this study and should be further investigated in a future study.

There are some limitations in the present study. First, the sample size was not large because of the rarity of RPLS. Second, this retrospective study was conducted at a single institution. Therefore, unexpected bias cannot be completely ruled out. Further prospective study, is needed in the future. Third, the intrarater reliability and interobserver variability of imaging analysis was not confirmed. Measurements of the CT value and ADC value in the tumor heavily depend on the operators that design the ROIs. Differences in imaging protocols may also have affected the image analyses. Further study is required to evaluate the usefulness of each modality in diagnosing RPLS.

Conclusion

This is the first study that compared the diagnostic accuracy of CT, PET, and MRI to survey high-grade conversion in intractable RPLS. The current study suggested that a contrast-enhanced CT value of 31 HU and an SUVmax of 2.9 on PET were helpful to identify dedifferentiated components with a satisfactory accuracy. Conflicting to our hypothesis, MRI was inferior to CT or PET for predicting DDLS and FNCLCC grade 2/3. We believe that these findings may help to design a surgical plan with a personalized approach, which attempts complete resection of dedifferentiated components with tumor-free margin. Additional research is needed in a large population to strengthen the evidence of the results observed in the current study.

Declarations

Conflict of interest The authors declare no conflict of interests.

References

- Matthysens LE, Creytens D, Ceelen WP (2015) Retroperitoneal liposarcoma: current insights in diagnosis and treatment. *Front Surg*. <https://doi.org/10.3389/fsurg.2015.00004>
- Brennan MF, Antonescu CR, Moraco N et al (2014) Lessons learned from the study of 10,000 patients with soft tissue sarcoma. *Ann Surg* 260(3):416–422
- Dehner CA, Hagemann IS, Chrisinger JSA (2021) Retroperitoneal dedifferentiated liposarcoma. *Am J Clin Pathol* 56(5):920–925
- Lahat G, Madewell JE, Anaya DA et al (2009) Computed tomography scan-driven selection of treatment for retroperitoneal liposarcoma histologic subtypes. *Cancer* 115(5):1081–1090
- Bhosale P, Wang J, Varma D et al (2016) Can abdominal computed tomography imaging help accurately identify a dedifferentiated component in a well-differentiated liposarcoma? *J Comput Assist Tomogr* 40(6):872–879
- Parkes A, Urquiola E, Bhosale P et al (2020) PET/CT imaging as a diagnostic tool in distinguishing well-differentiated versus dedifferentiated Liposarcoma. *Sarcoma*. <https://doi.org/10.1155/2020/8363986>
- Li CP, Liu DN, Zhou NN et al (2021) Prediction of histologic subtype and FNCLCC grade by SUVmax measured on 18F-FDG PET/CT in patients with retroperitoneal Liposarcoma. *Contrast Media Mol Imaging*. <https://doi.org/10.1155/2021/7191363>
- Subramaniam S, Callahan J, Bressel M et al (2021) The role of 18F-FDG PET/CT in retroperitoneal sarcomas—a multicenter retrospective study. *J Surg Oncol* 123(4):1081–1087
- Koh D-M, Collins DJ (2007) Diffusion-weighted MRI in the body: applications and challenges in oncology. *AJR Am J Roentgenol* 188(6):1622–1635
- Padhani AR, Liu G, Koh DM et al (2009) Diffusion-weighted magnetic resonance imaging as a cancer biomarker: consensus and recommendations. *Neoplasia* 11(2):102–125
- Bozgeyik Z, Onur MR, Poyraz AK (2013) The role of diffusion weighted magnetic resonance imaging in oncologic settings. *Quant Imaging Med Surg* 3(5):269–278
- Sbaraglia M, Bellan E, Dei Tos AP (2021) The 2020 WHO classification of soft tissue tumours: news and perspectives. *Pathologica* 113(2):70–84
- Guillou L, Coindre JM, Bonichon F et al (1997) Comparative study of the national cancer institute and French federation of cancer centers sarcoma group grading systems in a population of 410 adult patients with soft tissue sarcoma. *J Clin Oncol* 15(1):350–362
- Xue G, Wang Z, Li C et al (2021) A novel nomogram for predicting local recurrence-free survival after surgical resection for retroperitoneal liposarcoma from a Chinese tertiary cancer center. *Int J Clin Oncol* 26(1):145–153
- van Houdt WJ, Fiore M, Barretta F et al (2020) Patterns of recurrence and survival probability after second recurrence of retroperitoneal sarcoma: A study from TARPSWG. *Cancer* 126(22):4917–4925
- Gronchi A, Strauss DC, Miceli R et al (2016) Variability in patterns of recurrence after resection of primary retroperitoneal sarcoma (RPS): a report on 1007 patients from the multi-institutional collaborative rps working group. *Ann Surg* 263(5):1002–1009
- Singer S, Antonescu CR, Riedel E et al (2003) Histologic subtype and margin of resection predict pattern of recurrence and survival for retroperitoneal liposarcoma. *Ann Surg* 238(3):358–370
- Tseng WW, Madewell JE, Wei W et al (2014) Locoregional disease patterns in well-differentiated and dedifferentiated retroperitoneal liposarcoma: implications for the extent of resection? *Ann Surg Oncol* 21(7):2136–2143
- Jensen OM, Høgh J, Ostgaard SE et al (1991) Histopathological grading of soft tissue tumours prognostic significance in a prospective study of 278 consecutive cases. *J Pathol* 163(1):19–24

20. Neuhaus SJ, Barry P, Clark MA et al (2005) Surgical management of primary and recurrent retroperitoneal liposarcoma. *Br J Surg* 92(2):246–252
21. Linehan DC, Lewis JJ, Leung D et al (2000) Influence of biologic factors and anatomic site in completely resected liposarcoma. *J Clin Oncol* 18(8):1637–1643
22. Jha AK, Rodríguez JJ, Stopeck AT (2016) A maximum-likelihood method to estimate a single ADC value of lesions using diffusion MRI. *Magn Reson Med* 76(6):1919–1931
23. Walker-Samuel S, Orton M, Boulton JKR et al (2011) Improving apparent diffusion coefficient estimates and elucidating tumor heterogeneity using Bayesian adaptive smoothing. *Magn Reson Med* 65(2):438–447
24. Walker-Samuel S, Orton M, McPhail LD et al (2009) Robust estimation of the apparent diffusion coefficient (ADC) in heterogeneous solid tumors. *Magn Reson Med* 62(2):420–429
25. Muzaffar R, Koester E, Frye S et al (2020) Development of simple methods to reduce the exposure of the public to radiation from patients who have undergone 18F-FDG PET/CT. *J Nucl Med Technol* 48(1):63–67
26. Shaish H, Kang SK, Rosenkrantz AB (2017) The utility of quantitative ADC values for differentiating high-risk from low-risk prostate cancer: a systematic review and meta-analysis. *Abdom Radiol (NY)* 42(1):260–270
27. Hou B, Xiang S-F, Yao G-D et al (2014) Diagnostic significance of diffusion-weighted MRI in patients with cervical cancer: a meta-analysis. *Tumour Biol* 35(12):11761–11769
28. Gabelloni M, Faggioni L, Neri E (2019) Imaging biomarkers in upper gastrointestinal cancers. *BJR Open*. <https://doi.org/10.1259/bjro.20190001>
29. Schurink NW, Lambregts DMJ, Beets-Tan RGH (2019) Diffusion-weighted imaging in rectal cancer: current applications and future perspectives. *Br J Radiol* 92(1096):20180655
30. Satoh S, Kitazume Y, Ohdama S et al (2008) Can malignant and benign pulmonary nodules be differentiated with diffusion-weighted MRI? *AJR Am J Roentgenol* 191(2):464–470

Publisher's Note Springer Nature remains neutral with regard to jurisdictional claims in published maps and institutional affiliations.

Springer Nature or its licensor (e.g. a society or other partner) holds exclusive rights to this article under a publishing agreement with the author(s) or other rightsholder(s); author self-archiving of the accepted manuscript version of this article is solely governed by the terms of such publishing agreement and applicable law.